Two-scale modelling of reinforced concrete deep beams: Choice of unit cell and comparison with single-scale modelling

Advances in Engineering Materials, Structures and Systems: Innovations, Mechanics and Applications - Zingoni (Ed.)

Two-scale modelling of reinforced concrete deep beams: choice of unit cell and comparison with single-scale modelling

A. Sciegaj & A. Mathern
Department of Industrial and Materials Science, *Department of Architecture and Civil Engineering*,
Chalmers University of Technology, Gothenburg, Sweden

ABSTRACT: Two-scale and single-scale models are used to analyse the response of reinforced concrete deep beams with different reinforcement layouts. To this end, a novel approach of modelling non-uniformly reinforced structures in a multiscale manner is developed. Parameterised generation of suitable unit cells is described, and the subdivision of problem domain into regions with different substructures is presented. Three different reinforced concrete deep beams with available experimental data are analysed. Mid-span deflections are slightly underestimated by both models, while the maximum load is captured reasonably well.

1 INTRODUCTION

Nowadays a wide variety of analysis methods are available to structural engineers. Single-scale nonlinear finite element analysis is often presented as the most accurate method being able to capture cracking in detail. However, for large reinforced concrete structures, it often leads to big and complex models that are computationally too expensive. Multiscale modelling, specifically the FE^2 method provides an attractive alternative to conventional nonlinear finite element analysis, as accurate results can be obtained at a fraction of the single-scale analysis time. A two-scale model of reinforced concrete was developed (Sciegaj et al. 2018), wherein the cracking of concrete, plasticity of reinforcement and bond-slip interaction between the materials were taken into account.

However, the response of beams with non-uniform reinforcement layout has not been previously investigated. The model was also not validated by comparison with available experimental data.

In this contribution, several deep beams with available experimental data were analysed with both two- and single-scale models. A novel approach of modelling structures with non-uniform reinforcement layout in multiscale manner was employed, and a comparison with single-scale analyses was carried out. At this stage of the study only the force–deflection relation was examined. Of particular interest was the choice of a suitable unit cell, especially in regions where the reinforcement layout is not periodic. Lastly, it was also of interest to compare the performance of the two-scale analysis with single-scale modelling, both in terms of computational time, and the modelling effort.

2 PROBLEM FORMULATION

In this section, the governing partial differential equations, on which a finite element solution procedure can be built in both single and two-scale setting, are briefly outlined. For a detailed derivation the reader is kindly referred to (Sciegaj et al. 2018).

2.1 *Single-scale problem*

A reinforced concrete member in plane stress is considered. The thickness of the structure, t_c, is assumed to be much smaller than the other dimensions. The simplified two-dimensional domain Ω consists of the concrete part, Ω_c, and the reinforcement part, Γ_{int}, which is idealised as one-dimensional segments. The boundary of the domain Ω, which can be subjected to prescribed tractions $\hat{\boldsymbol{t}}$ or prescribed displacements, is denoted Γ_{ext}. The concrete is assumed to be a two-dimensional solid, for which momentum balance can be established. Only the longitudinal (bar) action is assumed for the reinforcement, whereby the normal force, N_s, can be related to the bond stress, $\boldsymbol{t}_\Gamma$, distributed along the perimeter of the bar, S_s. The quasi-static problem can then be summarised in the weak

forms as follows: find the concrete and reinforcement displacements $\boldsymbol{u}_{\mathrm{c}}, \boldsymbol{u}_{\mathrm{s,l}}$ that solve

$$\int_{\Omega_{\mathrm{c}}} t_{\mathrm{c}} \boldsymbol{\sigma}_{\mathrm{c}} : [\delta \boldsymbol{u}_{\mathrm{c}} \otimes \boldsymbol{\nabla}] \, \mathrm{d}\Omega - \int_{\Gamma_{\mathrm{int}}} S_{\mathrm{s}} \boldsymbol{t}_{\boldsymbol{\Gamma}} \boldsymbol{e}_l \delta \boldsymbol{u}_{\mathrm{c}} \mathrm{d}\Gamma = \int_{\Gamma_{\mathrm{ext}}} t_{\mathrm{c}} \hat{\boldsymbol{t}} \cdot \delta \boldsymbol{u}_{\mathrm{c}} \mathrm{d}\Gamma, \tag{1}$$

$$\int_{\Gamma_{\mathrm{int}}} N_{\mathrm{s}} \frac{\partial \delta \boldsymbol{u}_{\mathrm{s,l}}}{\partial l} \mathrm{d}\Gamma + \int_{\Gamma_{\mathrm{int}}} S_{\mathrm{s}} \boldsymbol{t}_{\boldsymbol{\Gamma}} \delta \boldsymbol{u}_{\mathrm{s,l}} \mathrm{d}\Gamma = 0, \tag{2}$$

for a suitable choice of test functions $\delta \boldsymbol{u}_{\mathrm{c}}$ and $\delta \boldsymbol{u}_{\mathrm{s,l}}$.

2.2 *Two-scale problem*

In this contribution, a coupled hierarchical multiscale method, more specifically the FE^2 method was employed. In this method, the total solution field is split into "smooth" and "fluctuation" parts, cf. (Larsson et al. 2010). As a result, the problem is divided into a large-scale domain Ω, which is considered to consist of the homogeneous material with "effective" properties, and the subscale domains, which reflect the underlying heterogeneity (and possibly randomness) of the material. The subscale problem follows directly from (1) and (2) upon restriction to a subscale unit cell (also called Representative Volume Element - RVE) domain, $\Omega_{\square}$. The "effective" response used in the large-scale problem is obtained from computational homogenisation of the response of the subscale unit cells. Classical first-order homogenisation is employed here, i.e. the gradient of the large-scale field is imposed on the unit cells via suitable boundary conditions (prolongation). In the case of the structural problem considered here, the gradient of the large-scale displacement, i.e. the effective strain was imposed on the RVE via Dirichlet boundary conditions, which means that the deformation of the boundary of the unit cell varied linearly. After solving the subscale problem, the effective properties are computed via averaging (homogenisation) and are transferred back to the large-scale. A schematic illustration of the FE^2 method is shown in Figure 1.

The large-scale problem can be expressed as: Find the effective displacement $\bar{\boldsymbol{u}}$ that solves:

$$\int_{\Omega} \bar{\boldsymbol{\sigma}} : [\delta \bar{\boldsymbol{u}} \otimes \boldsymbol{\nabla}] \, \mathrm{d}\Omega = \int_{\Gamma_{\mathrm{ext}}} t_{\mathrm{c}} \hat{\boldsymbol{t}} \cdot \delta \bar{\boldsymbol{u}} \mathrm{d}\Gamma, \tag{3}$$

where the effective stress $\bar{\boldsymbol{\sigma}}$ is computed from the subscale problem as:

$$\bar{\boldsymbol{\sigma}} = \frac{1}{|\Omega_{\square}|} \left[\int_{\Omega_{\square}} t_{\mathrm{c}} \boldsymbol{\sigma}_{\mathrm{c}} \mathrm{d}\Omega + \int_{\Gamma_{\square,\mathrm{int}}} N_{\mathrm{s}} \boldsymbol{e}_l \otimes \boldsymbol{e}_l \mathrm{d}\Gamma \right]. \tag{4}$$

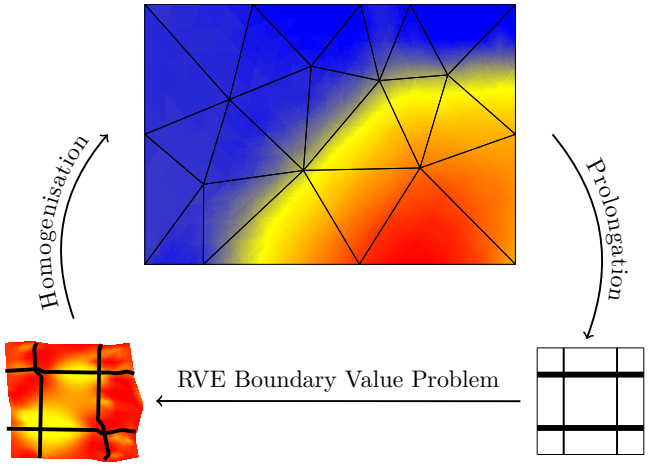

Figure 1: FE^2 scheme.

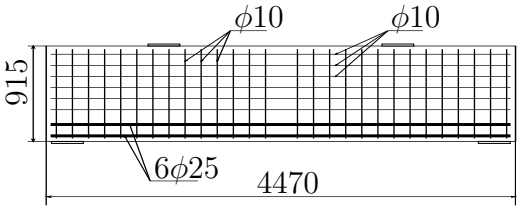

Figure 2: Dimensions and rebar layout for ACI-I beam.

Although theoretically each macroscopic point has an underlying microstructure, the numerical integration is performed at Gauss points. Hence, it suffices to introduce the unit cells only at the large-scale integration points

3 EXPERIMENTAL STUDIES

The FE^2 method described in previous section was successfully used in structural analysis of reinforced concrete members in plane stress, with uniform reinforcement pattern, cf. (Sciegaj et al. 2018, Sciegaj et al. 2019). In reality, the reinforcement can be concentrated in certain parts of the structural member. The described multiscale modelling technique was used to analyse three different deep beams of reinforced concrete, for which well-documented experimental results were available. The first two beams were named ACI-I and STM-M, cf. (Aguilar et al. 2002), whereas the third beam was named WT4, cf. (Leonhardt and Walther 1966). They are schematically depicted in Figures (2)–(4). For details regarding the test setup, the reader is referred to the given sources.

3.1 *ACI-I beam*

ACI-I consisted in a reinforced concrete member with a rather uniform reinforcement layout, i.e. a reinforcement grid in most part of the beam. However, it also had a distinct tie at the bottom in form of two rebars with considerably larger diameter than the rest. The beam was subjected to four-point bending. Reported compressive strength of concrete was 33 MPa, modu-

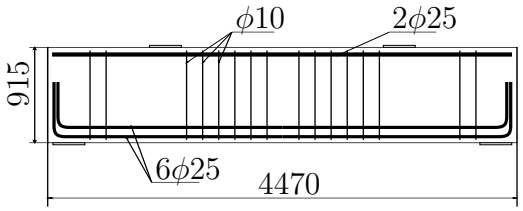

Figure 3: Dimensions and rebar layout for STM-M beam.

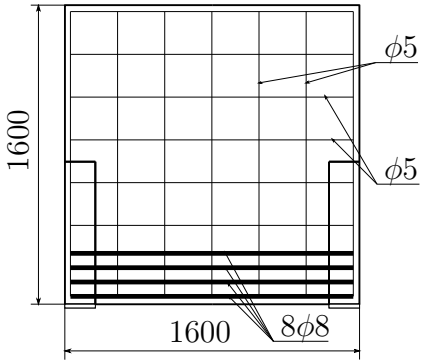

Figure 4: Dimensions and rebar layout for WT4 beam.

lus of rupture was 5 MPa (which was converted to a tensile strength of 3.34 MPa according to (Fib 2013)). The yield and ultimate strength for 25 mm bars were 420 MPa and 700 MPa, whereas the corresponding values for 10 mm rebars were 450 MPa and 720 MPa, respectively. The Young's modulus (32 GPa) and fracture energy (136.98 N/m) were obtained using the empirical formulas from Model Code 2010 (Fib 2013).

3.2 *STM-M beam*

STM-M had the same geometry and material properties for concrete and steel as ACI-I beam, except for the concrete compressive strength reported as 28 MPa. However, the reinforcement layout was hardly uniform as there was a distinct tie at the bottom of the beam and only a few stirrups were present. Like ACI-I, this beam was also subjected to four-point bending. Model Code 2010 (Fib 2013) empirical relations were used to calculate the Young's modulus (30.29 GPa) and fracture energy (132.99 N/m).

3.3 *WT4 beam*

The WT4 beam had a uniform reinforcement layout throughout the structure and a much lower span-to-depth ratio than the other beams. In addition to the regular reinforcement grid, a tie in form of several horizontal rebars concentrated at the bottom of the beam was present. In contrast to the previous beams, it was subjected to uniformly distributed load at the top surface. Reported compressive strength of concrete was 32.17 MPa. The yield strength of reinforcement was given as 415 MPa. Empirical formulas from Model Code 2010 (Fib 2013) were used to compute the Young's modulus (31.74 GPa), tensile strength (2.59 MPa) and the fracture energy (136.35 N/m).

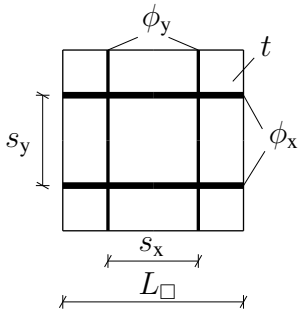

Figure 5: Generic unit cell, $\square$, and the input parameters.

4 COMPUTATIONAL MODELS

Two-scale simulations were performed using the open source C++ code OOFEM (Patzák 2012), while ABAQUS (Dassault Systèmes 2014) was used for single-scale analyses. The simulations were performed on a compute node with 20 core Intel 2650v3 CPU and 64 GB of RAM per node.

4.1 *Two-scale models*

Concrete and steel were modelled with bilinear quadrilateral and truss elements, respectively, while linear interface elements were used to simulate the bond between them. The rotating crack model with exponential softening in tension and linear elasticity in compression was used for concrete. For the steel, von Mises plasticity with linear hardening (ACI-I and STM-M beams) or perfect plasticity (WT4 beam) was used. The standard bond-slip relation given in Model Code 2010 (Fib 2013) was used for the interface. In order to build a two-scale model, it is necessary to find a suitable unit cell, which should reflect the subscale heterogeneity and randomness of the material in a good way. In case of reinforced concrete at this scale, the heterogeneity comes mainly from reinforcement distribution, hence it is necessary to be able to include arbitrary reinforcement layout within the RVE. Another important thing for the two-scale model is to divide the large-scale domain into regions, which will be represented by the same unit cell.

4.1.1 *Subscale unit cell generation*

A generic RVE can be seen in Figure (5). In order to make the generation of the subscale unit cell robust, the process was parameterised. An arbitrary (periodic) arrangement of the reinforcement can be reproduced by specifying the size of the RVE, $L_\square$, its thickness, t, amount of horizontal and vertical reinforcement (ϕ_x and ϕ_y, respectively), as well as the corresponding spacing between the rebars (s_y and s_x). Depending on the relation between the spacings and the side length, either one or more rebars can fit within the RVE. The shape of the unit cell was chosen to be a square, as it is usually done in practice. The sizes

Table 1: Unit cell geometry in FE^2 analyses of ACI-I beam.

		$L_\square$ mm	t mm	ϕ_x –	s_y mm	ϕ_y –	s_x mm
ACI-I1	$\square_1$	127	305	$3\phi25$	127	$2\phi10$	152.4
	$\square_2$	101.6	305	$2\phi10$	101.6	$2\phi10$	152.4
ACI-I2	$\square_1$	254	305	$3\phi25$	127	$2\phi10$	152.4
	$\square_2$	101.6	305	$2\phi10$	101.6	$2\phi10$	152.4

Table 2: Unit cell geometry in FE^2 analyses of STM-M beam.

		$L_\square$ mm	t mm	ϕ_x –	s_y mm	ϕ_y –	s_x mm
STM-M1	$\square_1$	101.6	305	$3\phi25$	101.6	$2\phi10$	152.4
	$\square_2$	152.4	305	–	–	$2\phi10$	152.4
	$\square_3$	152.4	305	$2\phi25$	152.4	$2\phi10$	152.4
	$\square_4$	101.6	305	$3\phi25$	101.6	–	–
	$\square_5$	101.6	305	$2\phi25$	101.6	–	–
	$\square_6$	101.6	305	–	–	–	–
STM-M2	$\square_1$	203.2	305	$3\phi25$	101.6	$2\phi10$	152.4
	$\square_2$	152.4	305	–	–	$2\phi10$	152.4
	$\square_3$	152.4	305	$2\phi25$	152.4	$2\phi10$	152.4
	$\square_4$	203.2	305	$3\phi25$	101.6	–	–
	$\square_5$	101.6	305	$2\phi25$	101.6	–	–
	$\square_6$	101.6	305	–	–	–	–

of the unit cells were chosen to be equal to a multiple of the spacing between rebars in one direction. Practical implication of this choice is that the periodicity of the reinforcement mesh is disrupted if the spacings s_x and s_y are different, which is often the case. To remedy this, the amount of reinforcement (area) was adjusted so that the amount of reinforcement per length is maintained between the RVEs. A number of unit cells was generated for each analysis, which are summarised in Tables (1)–(3). Depending on the RVE, the element size varied between 7.5 mm and 31.75 mm.

4.1.2 *Large-scale subdivision*

The reinforcement layout present in the structure should be reflected in the large-scale model by subdividing it into regions that correspond to specific unit cells. Although in theory, the size of the macroscopic elements may be quite large, this subdivision will restrain the maximum size of some elements. In case of uniformly distributed reinforcement the subdivision is quite straightforward, but with concentrated reinforcement/singular rebars this is a more delicate task.

Table 3: Unit cell geometry in FE^2 analyses of WT4 beam.

		$L_\square$ mm	t mm	ϕ_x –	s_y mm	ϕ_y –	s_x mm
WT4-1	$\square_1$	60	100	$2\phi8$	60	$2\phi5$	260
	$\square_2$	60	200	$2\phi8$	60	$2\phi5$	260
	$\square_3$	260	100	$2\phi5$	260	$2\phi5$	260
	$\square_4$	260	150	$2\phi5$	260	$2\phi5$	260
WT4-2	$\square_1$	120	100	$2\phi8$	60	$2\phi5$	260
	$\square_2$	120	200	$2\phi8$	60	$2\phi5$	260
	$\square_3$	260	100	$2\phi5$	260	$2\phi5$	260
	$\square_4$	260	150	$2\phi5$	260	$2\phi5$	260
WT4-3	$\square_1$	240	100	$2\phi8$	60	$2\phi5$	260
	$\square_2$	240	200	$2\phi8$	60	$2\phi5$	260
	$\square_3$	260	100	$2\phi5$	260	$2\phi5$	260
	$\square_4$	260	150	$2\phi5$	260	$2\phi5$	260

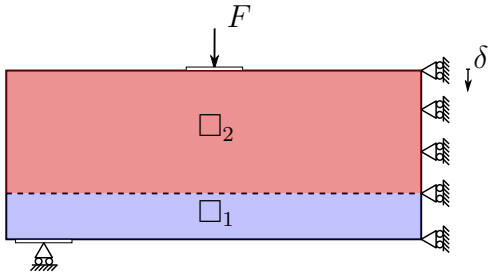

Figure 6: Subdivision of ACI-I beam into unit cell regions.

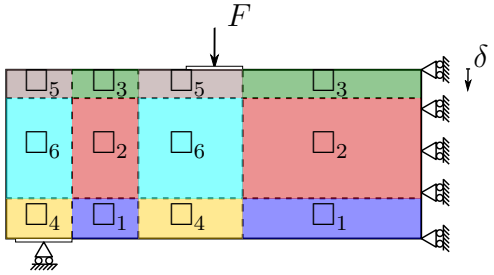

Figure 7: Subdivision of STM-M beam into unit cell regions.

The large-scale subdivisions are depicted for the three beams in Figures (6)–(8). The goal was to reflect the real reinforcement layout in the beam with fidelity. Special attention was given to concentrated reinforcement at the bottom of the beams. It should be noted that only half of each beam was modelled due to symmetry. The ACI-I and STM-M beams were subjected to concentrated forces, and therefore it was possible to run the analysis directly in displacement control by increasing the displacement under the loading platen gradually. WT4 beam was subjected to uniformly distributed load, hence it was decided to run the two-scale analysis in arc-length control.

4.2 *Single-scale models*

The single-scale analyses were conducted using static stress procedure (neglecting inertia effects) in ABAQUS/Standard (Dassault Systèmes 2014). Four-node bilinear plane stress quadrilateral (CPS4R) elements with reduced integration and hourglass control were used for the concrete. The reinforcing steel was modelled with 2-node linear truss (T2D2) elements

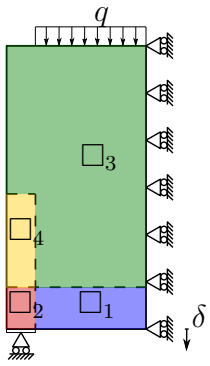

Figure 8: Subdivision of WT4 beam into unit cell regions.

embedded in the concrete, assuming perfect bond between the materials. An element size of 20 mm was used for the ACI-I and STM-M beams, while an element size of 25.4 mm was used for the WT4 beam. The Concrete Damaged Plasticity constitutive model available in ABAQUS was used to model the behaviour of concrete. The dilation angle was set to 30° and the viscosity parameter to 10^{-5}. Default values were used for the other plasticity parameters (i.e. 0.1 for the flow potential eccentricity, 1.16 for the biaxial to the uniaxial compressive strength ratio, and 0.67 for the tensile to compressive meridian ratio). Similar to two-scale models, linear elastic behaviour was defined for the concrete in compression. In tension, linear softening was employed, based on the fracture energy values. Steel was modelled assuming von Mises plasticity with linear hardening for the ACI-I and STM-M beams and perfect plasticity for WT4 beam based on the available test results. Displacement control (ACI-I and STM-M) and load control (WT4) were used for the analyses.

4.3 *Results and discussion*

The force–mid-span deflection relations for the beams are shown in Figures (9)–(11) for both two-scale and single-scale analyses. It is noteworthy, that the single- and two-scale analyses were performed independently of each other. Furthermore, even though different software and constitutive models were used, the results from the single-scale analyses agreed well with those from two-scale analyses in terms of force–displacement response. Moreover, the initial structural stiffness is well reflected by the simulations, and the predicted ultimate loads were close to those obtained in the experiments (error below 10 % for all analyses, except WT4-1 with an error below 15 %). Since no explicit (macroscopic) failure conditions were given in the models, the force–displacement response is given here up to the maximum deformation reported in the tests. The simulations continued past the reported data following the plastic response (except from single-scale analyses of ACI-I and STM-M beams, where a shear failure was observed at deformations a few millimetres larger than the experimental ones). There seems to be some additional deformation, measured in the experiments, which was not captured by the finite element models. This could be caused by the disparity between the "idealised" boundary conditions used in modelling and the real conditions of experiments setup, which are difficult to properly reproduce in a model.

It can be seen that the FE^2 simulations overestimated somewhat the structural response (for STM-M and WT4 beam), something that could be explained by the use of Dirichlet boundary conditions on the unit cells. The size of the unit cell in the critical regions of the beams (usually at the bottom) did not have much impact on the results for ACI-I and STM-M beam. It did, however, influence the maximum load prediction for the WT4 beam, with larger unit cell predicting lower load.

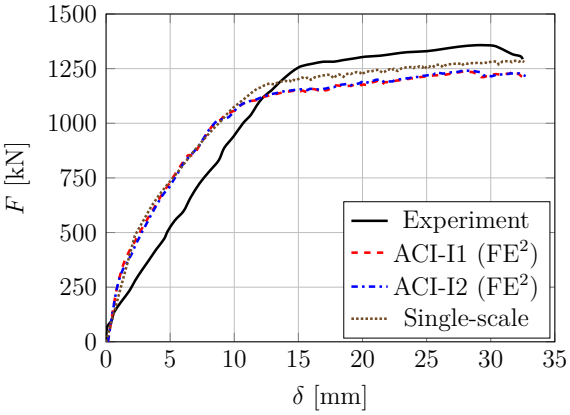

Figure 9: Force–mid-span deflection relation for ACI-I beam.

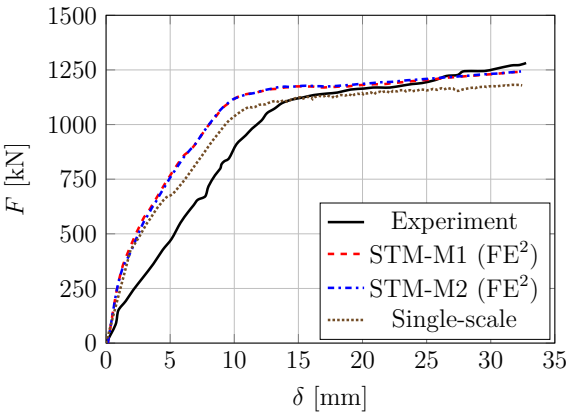

Figure 10: Force–mid-span deflection relation for STM-M beam.

The run-times of the analyses are presented in Table (4). For the studied beams, single-scale simulations were faster than their two-scale counterparts. However, it should be noted, that the two-scale implementation was not parallelised to allow for concurrent solution of different RVE problems. Hence, only a few of the available cores were used for the two-scale simulations. Regarding modelling complexity, the main difficulties in construction of two-scale mod-

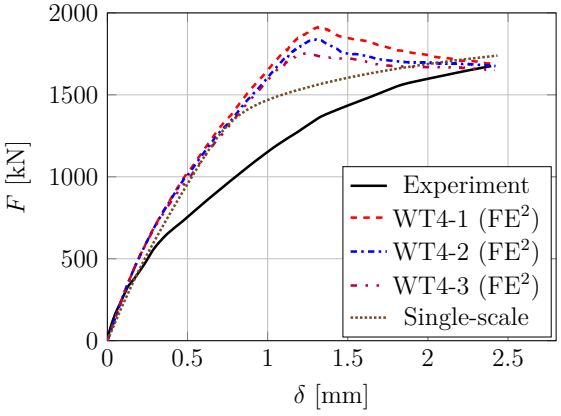

Figure 11: Force–mid-span deflection relation for WT4 beam.

Table 4: Run-times of the two-scale (FE^2) and single-scale analyses.

Analysis	Time [h]
ACI-I1 (FE^2)	01:38:10
ACI-I2 (FE^2)	06:51:16
ACI-I (Singe-scale)	01:09:02
STM-M1 (FE^2)	03:22:40
STM-M2 (FE^2)	08:14:00
STM-M (Single-scale)	00:42:59
WT4-1 (FE^2)	01:57:10
WT4-2 (FE^2)	02:42:50
WT4-3 (FE^2)	04:19:17
WT4 (Single-scale)	00:01:57

els of the beams comprise the choice of a suitable unit cell and appropriate subdivision of the large-scale domain. While the latter is a subtle geometric task, which might prove difficult for complex reinforcement layouts, the former can easily be parameterised allowing for efficient creation of generic unit cells, as long as reinforcement is arranged in a rectangular grid pattern. Single-scale simulations require more modelling effort, as every reinforcement bar had to be modelled separately. Moreover, allowing for bond-slip requires further modelling work, as the interface elements between steel and concrete need to be created.

5 CONCLUSIONS

In this contribution, a previously developed two-scale model of reinforced concrete was used for the first time to model several realistic examples of reinforced concrete deep beams with non-uniform reinforcement layouts. In the model, the response of concrete, steel, and the interface between them is considered in detail. Based on the formulation of the single-scale problem, the pertinent large-scale and subscale problems were outlined. The macroscopic variables (effective strain) were imposed on the subscale Representative Volume Elements (RVEs) with Dirichlet boundary conditions, and a procedure of computing the effective work conjugate (effective stress) was presented. A method of parameterised RVE generation was described, and the issue of large-scale subdivision was discussed.

Three reinforced concrete deep beams with different amounts and layouts of reinforcement were analysed both with two- and single-scale models. The main focus of the study was to investigate the feasibility of using a two-scale model when analysing structural members with non-uniform distribution of reinforcement. The ability of the model to capture force–deflection relations, choice of suitable unit cell, and appropriate large-scale subdivision were of special interest. Moreover, the performance of the multiscale method in terms of computational time and modelling complexity was compared to single-scale modelling.

Both types of analyses underestimated the deflection, while predicting the maximum load reasonably well. This slightly stiffer response could be caused by the fact, that certain deformations measured in the experiments were not reflected in the finite element models. In the FE^2 analyses, the size of the unit cell in crucial regions of the beams did not influence the force–deflection result much. Regarding computational performance, multiscale modelling provides an attractive alternative to conventional single-scale modelling in terms of modelling complexity. Potentially, this approach enables the study of large reinforced concrete structures, which would otherwise prove computationally far too expensive to handle in a single-scale manner.

For future work, the influence of the unit cell and large-scale subdivision on multiscale models should be studied closer. Also, developing further methods of including concentrated reinforcement in addition to uniformly distributed reinforcement might prove necessary. Furthermore, it is necessary to study the feasibility of multiscale methods to predict also other quantities, e.g. the crack widths and crack patterns, which can have a big impact on structural performance in the serviceability limit state. Finally, a larger number of experimentally studied structures needs to be examined in order to gain more insight.

REFERENCES

Aguilar, G., A. B. Matamoros, G. J. Parra-Montesinos, J. A. Ramirez, & J. K. Wight (2002). Experimental Evaluation of Design Procedures for Shear Strength of Deep Reinforced Concrete Beams. *ACI Structural Journal 99*(4), 539–548.

Dassault Systèmes (2014). Abaqus 6.14 Theory Manual. Technical report.

Fib (2013). *Model code for concrete structures 2010*. Wiley-VCH Verlag GmbH & Co. KGaA.

Larsson, F., K. Runesson, & F. Su (2010). Variationally consistent computational homogenization of transient heat flow. *International Journal for Numerical Methods in Engineering 81*(13), 1659–1686.

Leonhardt, F. & R. Walther (1966). Wandartige Träger. Heft 178. Technical report, Deutscher Ausschuss für Stahlbeton, Berlin.

Patzák, B. (2012). OOFEM - an object-oriented simulation tool for advanced modeling of materials and structures. *Acta Polytechnica 52*(6), 59–66.

Sciegaj, A., F. Larsson, K. Lundgren, F. Nilenius, & K. Runesson (2018). Two–scale finite element modelling of reinforced concrete structures: Effective response and subscale fracture development. *International Journal for Numerical Methods in Engineering 114*(10), 1074–1102.

Sciegaj, A., F. Larsson, K. Lundgren, F. Nilenius, & K. Runesson (2019). A multiscale model for reinforced concrete with macroscopic variation of reinforcement slip. *Computational Mechanics 63*(2), 139–158.